WAVEFORM DESIGN FOR LOW FREQUENCY SYNTHETIC APERTURE SONAR

Yan Pailhas[a]

[a]NATO STO Centre for Maritime Research and Experimentation

Viale S. Bartolomeo 400, 19126 La Spezia, Italy
email: yan.pailhas@cmre.nato.int

Abstract: *Wideband sonars effectively utilise their bandwidth to provide high resolution in range. In most cases, wideband sonar waveforms are LFM (Linear Frequency Modulated) pulses or linear chirps. For a linear chirp, the instantaneous frequency varies linearly with time. The range resolution signal is obtained through pulse compression or matched filtering. It is well known that the resulting range resolution is inversely proportional to the bandwidth Δf, and that the gain after pulse compression is the product of the bandwidth Δf and the pulse duration τ. In this talk, we will study the case of Quadratic Frequency Modulated (QFM) pulses. We will first derive the matched filtered response of this particular pulse and show that the range resolution and the power gain is similar to the LFM case. However we will illustrate that QFM presents a non-constant energy distribution in frequency which can be utilised to compensate the transducer energy loss at the lower end of the spectra. QFM can then be used to normalise the overall pulse energy without loss in the SNR (Signal to Noise Ratio). We will also demonstrate that in the case of SAS (Synthetic Aperture Sonar) systems and in particular in the case of low frequency SAS, quadratic frequency modulated pulses provide more robustness toward navigation errors and that the resulting PSF (Point Spread Function) is less susceptible to blurring effects.*

Keywords: *LFSAS, Waveform design.*

1. INTRODUCTION

The pulse of choice for sonar or radar systems has often been the LFM (Linear Frequency Modulated) waveform, as it offers interesting characteristics in terms of range estimation and SNR (Signal-to-Noise Ratio) gain thanks to pulse compression. The use of high order PFM (Polynomial Frequency Modulated) waveforms with a non linear instantaneous frequency has also been of interest for the study of brown bat signals, frequency tracking algorithms [1], underwater communications [2] or image reconstruction algorithms for ISAR (Inverse Synthetic Aperture Radar) for targets with high manoeuvrability capabilities [3]. The PFMs ambiguity function has also been studied for SAR (Synthetic Aperture Radar) applications, PFM waveforms can provide a lower SNR threshold for target detection and better capability to discriminate multiple components signals [4]. As part of the HRLFSAS (High Resolution Low Frequency Synthetic Aperture Sonar) project [5], we investigate in this paper the use of PFM and in particular QFM (Quadratic Frequency Modulated) waveforms for low frequency systems. Low frequency ultra wideband systems can represent a great challenge in terms of engineering [6] as low frequencies require greater efforts to produce. We will show that QFM presents a non-uniform frequency spectra which can be utilised to increase the output energy at the lower end of the spectra.

2. POLYNOMIAL FREQUENCY MODULATED WAVEFORMS

2.1. LFM

In this paper, we are considering polynomial frequency modulated pulses $s(t)$ of the form

$$s(t) = A(t)\exp\left[2i\pi\left(f_1 t + \frac{t^k \Delta f}{k\tau^{k-1}}\right)\right], \tag{1}$$

for $t \in [0,\tau]$ and with $k \in \mathbb{N}^*$. In (1), Δf represents the bandwidth, f_1 the starting frequency, τ the pulse duration and $A(t)$ the windowing or weighting function. For $k = 2$, we obtain

$$s(t) = A(t)\exp\left[2i\pi\left(f_1 t + \frac{t^2 \Delta f}{2\tau}\right)\right], \tag{2}$$

which represents the classical formula for LFM (Linear Frequency Modulated) pulses. Range resolution is then obtained by cross-correlation between the received signal and the transmitted signal. The matched filter response $s_{MF}(t)$ is then given by

$$s_{MF}(t) = \int_{-\infty}^{+\infty} s^*(t)s(t'+t)dt'. \tag{3}$$

In radar, due to physical and electronic constraints, the windowing function $A(t)$ is most of the time a rectangular window. The analytical solution of (3) in that case is well known [7] and writes

$$s_{MF}(t) = \tau\frac{\sin[\pi t\Delta f(1-|t|/\tau)]}{\pi t\Delta f}\exp(2i\pi f_0 t), \tag{4}$$

where $f_0 = f_1 + \Delta f/2$ is the central frequency. For a Gaussian window with $A(t) = \exp\left[-\frac{(t-\tau/2)^2}{2\sigma^2}\right]$, the analytical solution to (3) also exists [8] and writes as

$$s_{MF}(t) = \sigma\sqrt{\pi}\exp\left[-\left(\frac{1}{4\sigma^2} + \frac{\pi^2\Delta f^2\sigma^2}{\tau^2}\right)t^2\right]\exp(2i\pi f_0 t). \tag{5}$$

2.2. QFM

Following the same notations as in section 2.1, a QFM pulse $s(t)$ corresponds to $k = 3$ in Eq. (1) and writes

$$s(t) = A(t)\exp\left[2i\pi\left(f_1 t + \frac{t^3\Delta f}{3\tau^2}\right)\right]. \tag{6}$$

Note that the instantaneous frequency corresponding to the time derivative of the phase $\varphi(t)$ of $s(t)$ divided by 2π is now a quadratic function as observed in Eq. (7).

$$\varphi'(t) = 2\pi(f_1 + \Delta f\tau^{-2}t^2) \tag{7}$$

The same Gaussian windowing function $A(t)$ as in 2.1 will be used for the derivation of $s_{MF}(t)$. Using (6) into (3) leads to

$$s_{MF}(t) = \exp\left(-\frac{\tau^2}{8\sigma^2}\right)s(t)\int_{-\infty}^{+\infty}\exp\left[-\left(\frac{1}{\sigma^2} - 2i\pi\frac{\Delta f}{\tau^2}t\right)t'^2 + \left(-\frac{t-\tau}{\sigma^2} + 2i\pi\frac{\Delta f}{\tau^2}t^2\right)t'\right]dt'. \tag{8}$$

Let

$$a = \frac{1}{\sigma^2} - 2i\pi\frac{\Delta f}{\tau^2}t \;\text{ and }\; b = -\frac{t-\tau}{\sigma^2} + 2i\pi\frac{\Delta f}{\tau^2}t^2. \tag{9}$$

The integral of the righthand side of (8) then becomes

$$\int_{-\infty}^{+\infty}\exp\left(-ax^2 + bx\right)dx = \sqrt{\frac{\pi}{a}}\exp\left(\frac{b^2}{4a}\right). \tag{10}$$

Note that the resolution of the complex Gaussian integral [9] is valid for all $a, b \in \mathbb{C}^*$. Let now define

$$\alpha = 2i\pi\frac{\Delta f}{\tau^2} \;\text{ and }\; \beta = \frac{1}{\alpha\sigma^2}. \tag{11}$$

It is interesting to note that $\alpha\beta = \frac{1}{\sigma^2}$. By combining (9) and (11), we arrive to

$$a = \alpha(\beta - t) \;\text{ and }\; b = \alpha(t^2 - \beta t + \beta\tau). \tag{12}$$

We can now derive the argument of the exponential function in (10) using a polynomial division

$$\frac{b^2}{4a} = \frac{\alpha}{4}\left[-t^3 + \beta(t-\tau)^2 - \beta\tau^2 + \frac{\beta^2\tau^2}{\beta - t}\right]. \tag{13}$$

Using the notations given by (13), the QFM pulse in (6) rewrites as

$$s(t) = \exp\left[-\frac{(t-\tau/2)^2}{2\sigma^2} + 2i\pi f_1 t + \frac{\alpha}{3}t^3\right]. \tag{14}$$

The exact analytical solution to (3) is then obtained by substituting (14) and (13) into (8):

$$s_{MF}(t) = \exp\left(-\frac{\tau^2}{8\sigma^2}\right)\exp\left[\frac{\alpha}{12}t^3 - \frac{t^2}{4\sigma^2} + \frac{\tau^2}{8\sigma^2} + 2i\pi f_1 t + \frac{\alpha}{4}\frac{\beta\tau^2}{1-t/\beta}\right]. \tag{15}$$

Eq. (15) gives the exact solution to (8), its direct physical interpretation however is rather complex due to the last fractional term. A more comprehensive result is given by performing a Taylor expansion at the second order on (15) which leads to

$$s_{MF}(t) \approx \sigma\sqrt{\pi}\exp\left[-\left(\frac{1}{4\sigma^2} + \frac{\pi^2\Delta f^2\sigma^2}{\tau^2}\right)t^2\right]\exp\left[2i\pi\left(f_1 + \frac{\Delta f}{4}\right)t + 2i\pi\frac{\Delta f}{12\tau^2}t^3\right]. \tag{16}$$

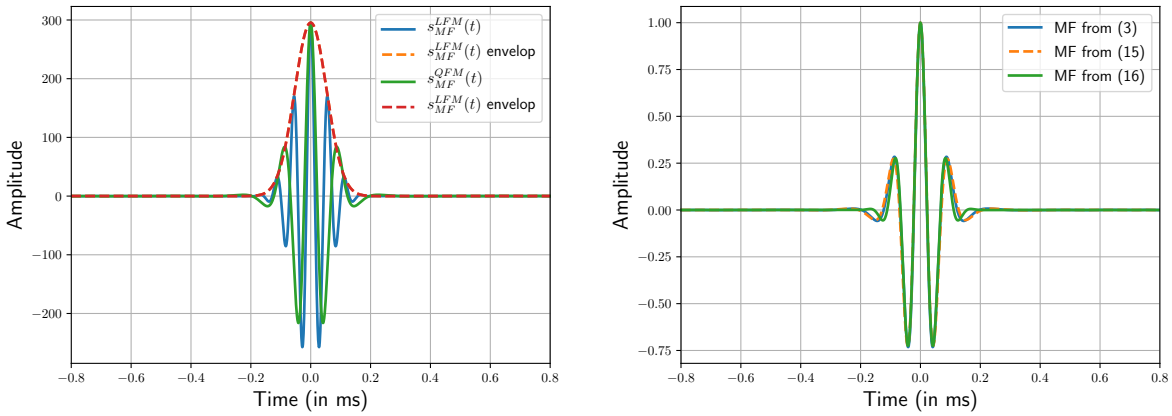

(a) (b)

Fig. 1: (a) *Matched filter responses of the LFM and the QFM with their respective envelopes.* (b) *Comparison between the matched filter responses of the QFM computed with the numerical method from* (3)*, the exact expression* (15) *and the approximation* (16)*.*

The comparison between the two matched filter responses (5) and (16) is particularly interesting. First, the amplification gain factor is identical and equals to $\sigma\sqrt{\pi}$ in both cases. Furthermore, the normalised amplitude envelope represented by the Gaussian term is also the same for both matched filter responses, meaning that range resolution as defined as the scatterer energy diffusion as in [8] is also identical for both waveforms. Thus, LFM and QFM Gaussian windowed waveforms provide through auto-correlation the same range resolution. The only difference between (5) and (16) lays in the phase of the function and is easily extracted from the last term in (16). Given that the width of $s_{MF}(t)$ is much smaller that the pulse duration τ, the cubic behaviour of the phase in (16) does not have a meaningful impact on the overall phase behaviour. At this point the only remaining difference lays in the apparent central frequency respectively $f_1 + \frac{\Delta f}{2}$ and $f_1 + \frac{\Delta f}{4}$ for the LFM and the QFM waveform. For a high frequency system such as the CMRE MUSCLE, $f_1 = 270$ kHz and $\Delta f = 60$ kHz. The central frequency after matched filtering will then be respectively 300 kHz and 285 kHz using a LFM and a QFM pulse. The 15 kHz difference at 300 kHz will not impact significantly the backscattered response nor the final sonar image. Considering now a low frequency system with $f_1 = 5$ kHz and $\Delta f = 20$ kHz. In that example, the central frequency of the QFM waveform will be lowered by a third of an octave compared to the LFM waveform, *i. e.* from 15 kHz down to 10 kHz.

For the next examples, the parameters for all waveforms (either LFM or QFM) are: $f_1 = 5$ kHz, $\Delta f = 20$ kHz, $\tau = 2$ ms and $\sigma = 4.10^{-4}$ s. In figure 1(a), we plotted the matched filter responses of a LFM and a QFM waveforms alongside their respective envelopes. As expected from the comparison between (5) and (16), both responses have the same maximum amplitude and the same envelope. The two envelopes actually superimpose perfectly. Figure 1(b) draws the matched filter response for a QFM pulse using the direct computation of the convolution as in (3), the exact analytical solution from (15) and the approximation response as written in (16). The figure shows that the approximation analytical solution (16) follows extremely closely the exact solution (15) with a small deviation in the sidelobes of the response which are not taken into account by the Taylor expansion at this order.

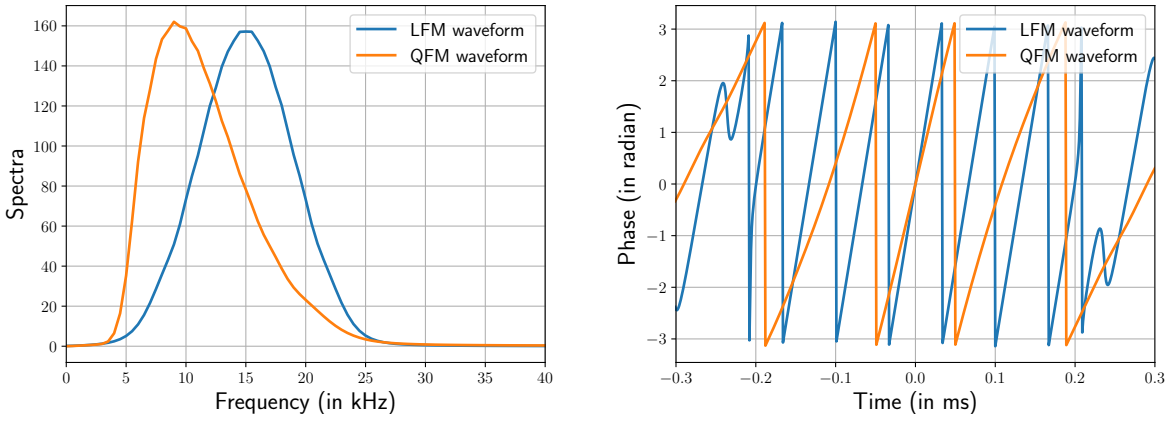

(a) (b)

Fig. 2: (a) *Spectra of the LFM and QFM matched filter responses.* (b) *Phase of the matched filter response of the LFM and QFM waveforms.*

Using the same pulse parameters, figure 2(a) plots the two spectra of the LFM and the QFM matched filter responses. As it has been highlighted previously, we observe a significant energy shift toward the lower frequency for the QFM response compared with the LFM response. A direct consequence of this energy shift can be spotted in figure 1(b) where the phase of the matched filter responses for the LFM and QFM pulses has been drawn. Note that the energy of both $s_{MF}(t)$ is concentrated in the time window $t \in$ [-0.2, 0.2] ms. Because the apparent central frequency of $s_{MF}^{QFM}(t)$ is significantly lower that the one of $s_{MF}^{LFM}(t)$ for low frequency systems, the phase variation is then significantly slower as seen in figure 2(b). In essence SAS processing consists in coherently summing matched filter echo responses. Decorrelation can come from imprecise estimation of the navigation (*i.e.* the precise localisation of the system when transmitting and receiving). A slower phase variation then provides more robustness to navigation errors.

3. CONCLUSIONS

In this paper, we derived the analytical formula for the matched filter response of a quadratic frequency modulated waveforms. For Gaussian windowed pulses and compared to LFM waveforms, QLMs offer the same amplitude gain and the same range resolution. The energy shift toward the lower frequencies however can represent an asset for low frequency systems as it

can concentrate the energy (and then offer a better SNR) on the lower part of the system's bandwidth. For SAS system, QLM waveforms also provide more robustness toward navigation errors.

ACKNOWLEDGEMENT

This work was performed under the Project SAC000905–High Resolution Low Frequency Synthetic Aperture Sonar (HRLFSAS) of the STO-CMRE Programme of Work, funded by the NATO Allied Command Transformation.

REFERENCES

[1] S. S. Abeysekera. Performance analysis of an autocorrelation based frequency tracker for LFM and QFM signals. In *2009 7th International Conference on Information, Communications and Signal Processing (ICICS)*, pages 1–5, Dec 2009.

[2] A. C. Pecci, C. Laot, and A. Bourre. Quadratic chirp modulation for underwater acoustic digital communications. In *OCEANS 2015 - Genova*, pages 1–7, May 2015.

[3] Y. Wang and Y. Jiang. Inverse synthetic aperture radar imaging of maneuvering target based on the product generalized cubic phase function. *IEEE Geoscience and Remote Sensing Letters*, 8(5):958–962, Sep. 2011.

[4] S. Barbarossa and V. Petrone. Analysis of polynomial-phase signals by the integrated generalized ambiguity function. *IEEE Transactions on Signal Processing*, 45(2):316–327, Feb 1997.

[5] Y. Pailhas, S. Fioravanti, and S. Dugelay. The high resolution low frequency synthetic aperture sonar (HR-LFSAS) project. In *SAR/SAS conference, Institute of Acoustics*, volume 40, pages 66–72, 2018.

[6] S. Fioravanti, F. Aglietti, A. Carta, A. Sapienza, and Y. Pailhas. Modular design of a 2D transmitting array for an advance low frequency synthetic aperture sonar. In *OCEANS 2019 - MTS/IEEE Marseille*, pages 1–6, Jun 2019.

[7] M. Cheney and B. Borden. *Fundamentals of Radar Imaging*. pp. 149. Society for Industrial and Applied Mathematics, Philadelphia, US, 2008.

[8] Y. Pailhas, Y. Petillot, and B. Mulgrew. Increasing circular synthetic aperture sonar resolution via adapted wave atoms deconvolution. *J. Acoust. Soc. Am.*, 141(4):2623–2632, 2017.

[9] A Zee. *Quantum Field Theory in a Nutshell*. pp. 576. Nutshell handbook. Princeton Univ. Press, Princeton, NJ, 2003.